Electronic Supplementary Material (ESI) for Green Chemistry.
This journal is © The Royal Society of Chemistry 2019

Supporting information

Sustainable biochar catalyst synergized with copper heteroatoms and CO_2 for singlet oxygenation and electron transfer routes

Zhonghao Wan[1], Yuqing Sun[1], Daniel C.W. Tsang[1, *], Iris K.M. Yu[1,2], Jiajun Fan[2], James H. Clark[2], Yaoyu Zhou[1,3], Xinde Cao[4], Bin Gao[5], Yong Sik Ok[6]

[1] *Department of Civil and Environmental Engineering, The Hong Kong Polytechnic University, Hong Kong, China*

[2] *Green Chemistry Centre of Excellence, Department of Chemistry, The University of York, York YO10 5DD, UK*

[3] *Hunan International Scientific and Technological Cooperation Base of Agricultural Typical Pollution Remediation and Wetland Protection, College of Resources and Environment, Hunan Agricultural University, Changsha 410128, China*

[4] *School of Environmental Science and Engineering, Shanghai Jiao Tong University, Shanghai 200240, PR China*

[5] *Department of Agricultural and Biological Engineering, University of Florida, Gainesville, FL 32611, United States*

[6] *Korea Biochar Research Centre & Division of Environmental Science and Ecological Engineering, Korea University, Seoul, South Korea*

* Corresponding author email: dan.tsang@polyu.edu.hk

The supporting information included:

6 Texts

18 Figures

20 Pages

Text S1. Chemical reagents

Cupric chloride dihydrate ($CuCl_2$•$2H_2O$), sodium peroxydisulfate ($Na_2S_2O_8$, PDS), glycerol ($C_3H_8O_3$), Rhodamine B ($C_{28}H_{31}ClN_2O_3$, RB), 4-chlorophenol (C_6H_5ClO, 4-CH), EDTA ($C_{10}H_{16}N_2O_8$), Fe_3O_4, Fe_2O_3, ZVI, CuO, CoO, MnO_2, and ZnO were purchased form Sigma-Aldrich Co., Ltd., USA. Phenol (C_6H_5OH, PN), bisphenol A ($C_{15}H_{16}O_2$, BPA), ethyl alcohol (C_2H_6O, EtOH), tert-Butanol ($C_4H_{10}O$, TBA), potassium iodide (KI), sodium bicarbonate ($NaHCO_3$), sodium hydroxide (NaOH), sodium chloride (NaCl), sodium nitrate ($NaNO_2$), concentrated nitric acid (HNO_3), acetone (C_3H_6O), acetonitrile (C_2H_3N), furfuryl alcohol ($C_5H_6O_2$, FFA), and chloroform ($CHCl_3$, CF) were obtained from Aladdin Chemical Reagent Co., Ltd., China. Graphene oxide was prepared by a modified Hummers method.[1]

Text S2. Microscopic characterization of Cu-BC composites

The Brunauer-Emmett-Teller (BET) surface area and Barrett-Joyner-Halenda (BJH) porosity analyses of the BC and Cu-BC composites were measured by using a surface analyzer (TriStar-II 3020, USA), and the samples were degassed at 90 °C for 16 h prior to the analysis. Morphology and elemental composition were observed by scanning electron microscopy-energy dispersive X-ray spectroscopy (SEM-EDX) (JSM-IT300, JXA-8230, Japan) operated at 20 kV. Reliability and consistency were maintained by using the binding energy at 284.8 eV of C 1s peak as a reference and strictly fixing all peak positions and the corresponding FWHMs based on the literature, although such practice may result in small deviation from raw data. The transmission electron microscopy (TEM) images were obtained from a JEOL JEM-2100 with an X-ray detector of Oxford INCA Energy TEM 100 (JEOL, Japan). High-resolution-powered X-ray diffraction (XRD) (Advance diffractometer, Germany) analysis was performed to identify the mineral phases and the

presence of carbon by using CuKa (λ = 1.54059 Å) radiation with a scanning range of 10° – 80° 2θ at 5° min^{-1}, at 45 kV and 200 mA. Raman spectra were recorded under ambient conditions using a confocal micro-Raman spectrometer (Renishwa Invia Fellex, UK) equipped with a Diode-Pumped Solid State (DPSS) laser source emitting at 532 nm. Fourier transform infrared spectroscopy (FTIR) (Nicolet 6700 spectrometer, USA) with the wavenumber ranging from 400 to 4000 cm^{-1} was used to identify the major near-surface bond groups of the samples. Thermogravimetric analysis (TGA) (Discovery TGA, USA) was performed from 100 °C to 1000 °C at a heating rate of 10 °C min^{-1} with Ar stripping gas. X-ray photoelectron spectroscopy (XPS) (ESCALAB 250Xi spectrometer, USA) with Al Kα radiation was used to investigate the composition and chemical state of the elements on the sample surfaces. Narrow high-resolution scans of C_{1s}, O_{1s}, and Cu_{2p}, were obtained using 25 eV pass energy with a step size of 0.05 eV. The charge effect was corrected by using the C 1s line at 284.8 eV. The obtained spectra were fitted by using a curve-fitting program (XPSPEAK41) and a least-squares procedure with peaks of 30% of the Lorentzian-Gaussian peak shape after subtraction of the Shirley baseline. The component peaks were identified by comparison of their binding energies (BEs) with the reported literature values.

Text S3. Extraction of metals and phenolic compounds

The metals and phenolic compounds were extracted by EDTA and glycerol, respectively, according to a method developed in previous studies.[2] Briefly, a certain amount of Cu-BC (*i.e.*, 1 g) or raw biomass (*i.e.*, 5 g) was mixed with 120mM EDTA or 40mM glycerol in 500-mL beakers under rigorously stirring for 2 h at 80 °C. After filtration, the phenol-free biomass was oven-dried overnight and pyrolyzed for BC production (denoted as G-BC). The treated Cu-BC (denoted as

EDTA-BC) was used for catalytic degradation.

Text S4. Two-chamber reactor

Two individual 200-mL chambers, *i.e.* anode chamber (organic pollutant) and cathode chamber (PDS), were physically separated by proton exchange membrane (PEM) and wire-connected between two electrodes (*i.e.*, carbon fiber brushes). The carbon fiber brushes were immersed in 1 mM HCl and 1 mM NaOH, respectively, for 12 h, and then rinsed with MW before storage for later use. The PEM (10 cm × 10 cm) was immersed in H_2SO_4 (5%, v/v) at 80 °C for 2 h and rinsed with MW before storage in desiccator.

Text S5. Analytical methods

The RB concentration was measured using a UV spectrophotometer (UV-1100, China) at a maximum wavelength of 554 nm. The concentrations of PH, BPA, and 4-CH were analyzed by a high-performance liquid chromatography (HPLC, Hitachi, Japan) equipped with a C-18 column (Eclipse XDB-C18) and a UV-VIS Detector. The concentrations of PH, BPA, and 4-CH were analyzed at 270, 280, and 280 nm, respectively. The mobile phase was a mixture of methanol (1.5 wt.%) and acetic acid with volume ratio of 60/40, 75/25, and 70/30, respectively, at a flow rate of 400 mL min^{-1}.

The PDS concentration was determined using a modified iodide oxidation method.[3] A chromogenic reagent containing 1,000 g L^{-1} KI and 5 g L^{-1} $NaHCO_3$ was prepared. The reagent was allowed to equilibrate for 15 min, and then 10-mL reagent was transferred into a 15-mL polypropylene centrifuge tube. An aliquot of 0.25-mL sample from a batch test was added to the tube, and then the mixture was thoroughly mixed for a few seconds and allowed to stand for 20

min. The solution was yellow and absorbance was measured at a wavelength of 352 nm using an Optizen Pop UV-Vis spectrometer.

The electron spin resonance (ESR) spectra were obtained using an EMX10/12 spectrometer (EMX10/12, Bruker, Germany). The instrument conditions were as follows: resonance frequency of 9.82 GHz, microwave power of 20.07 mW, modulation frequency of 100 kHz, modulation amplitude of 1.0 G, sweep width of 100 G, time constant of 40.96 ms, sweep time of 83.93 s, and receiver gain of 2.0×10^4 at room temperature. In the sample vials, 150 mM 5,5-dimethyl-1-pyrroline-N-oxide (DMPO) or 2, 2, 6, 6-tetramethyl-4-piperidinol (TEMP) was added as the spin-trapping agent in a buffer solution (pH = 7.4, 20mM phosphate). Peak intensities of the DMPO–SO_4, DMPO–OH, and TEMPN signals at 5 min were applied as indexes of the generated ROS after the correction of background noise.

Text S6. Regeneration methods

Three catalyst regeneration methods were evaluated in preliminary experiments, including conventional thermal annealing (ramping to 300 °C at a rate of 5 °C min^{-1} and holding for 2 h in a muffle furnace in air atmosphere), sonication (10 min at room temperature), and chemical desorption (acetonitrile or acetone at solid/liquid ratio of 1 g per 100 mL for 5 min). Results showed that thermal annealing was not applicable for the regeneration of Cu-GBC. The annealed carbocatalyst exhibited unfavorable catalytic activity possibly due to the oxidation of copper atoms disrupting the Cu–O–C matrix, and the increased oxygen level might also affect the reducibility of carbon framework. Sonication was also not effective as exfoliation of copper layer may occur, leading to the severe loss of accessible active sites. Besides, the re-adsorption of intermediates after sonication might account for the poor regeneration efficiency. Chemical desorption showed

the highest regeneration efficiency, in which acetonitrile or acetone could maintain 70–80% catalytic efficiency in the fourth run. The Cu-GBC may behave like both 'geobattery' and 'geoconductor' similar to the high-temperature pyrogenic carbon previously reported, and redox recycling and charge transfer could be fulfilled simultaneously.[4] We selected acetone in this study in view of its lower toxicity compared to acetonitrile.

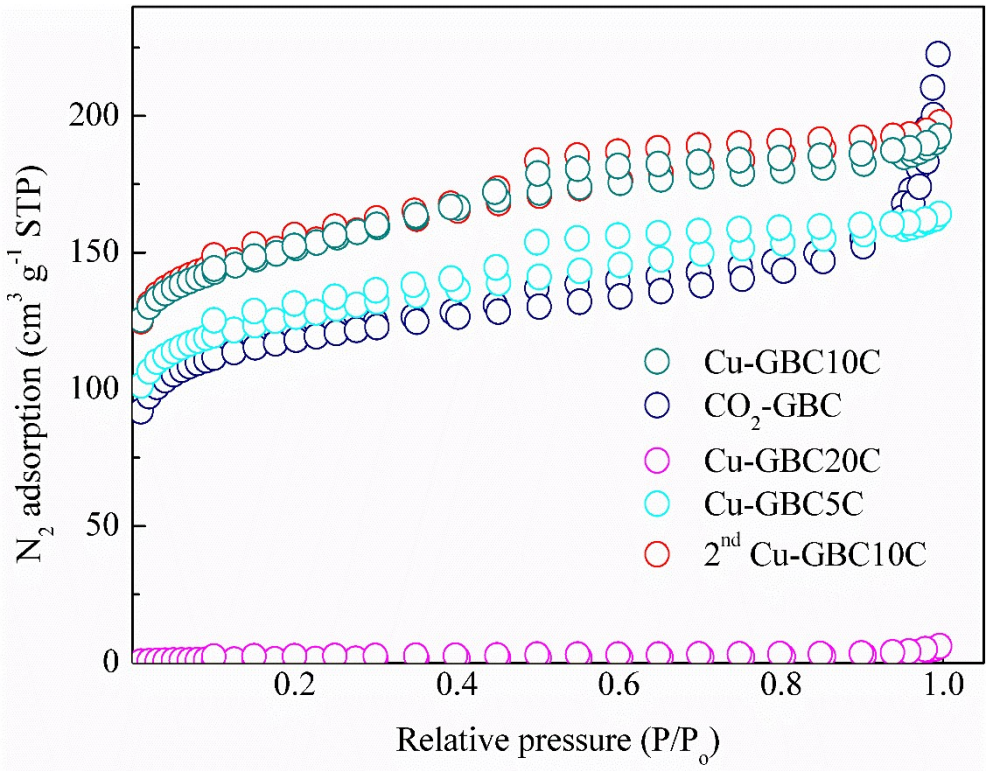

Fig. S1. N_2 adsorption-desorption isotherms of various biochar composites.

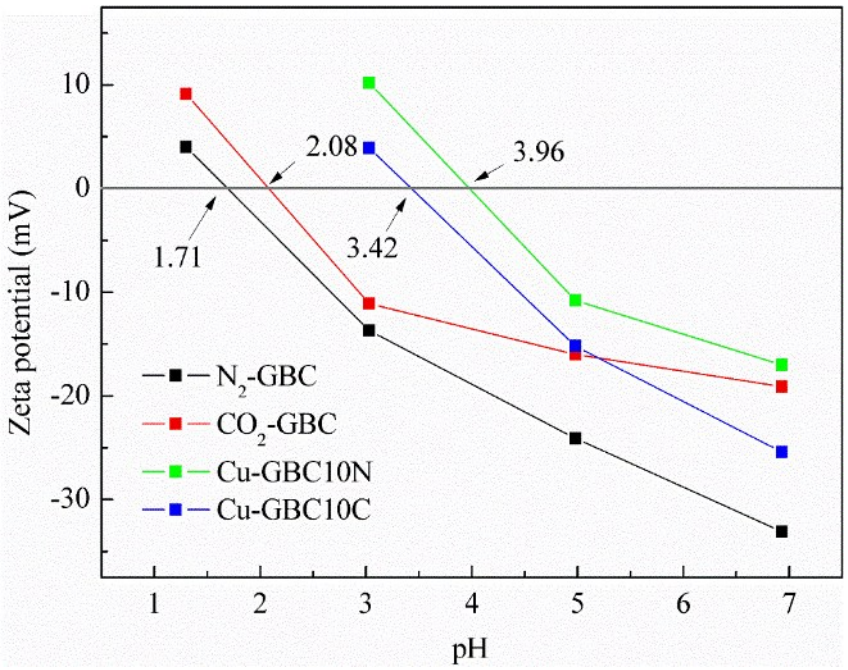

Fig. S2. Determination of pH_{pzc} values of various biochar composites.

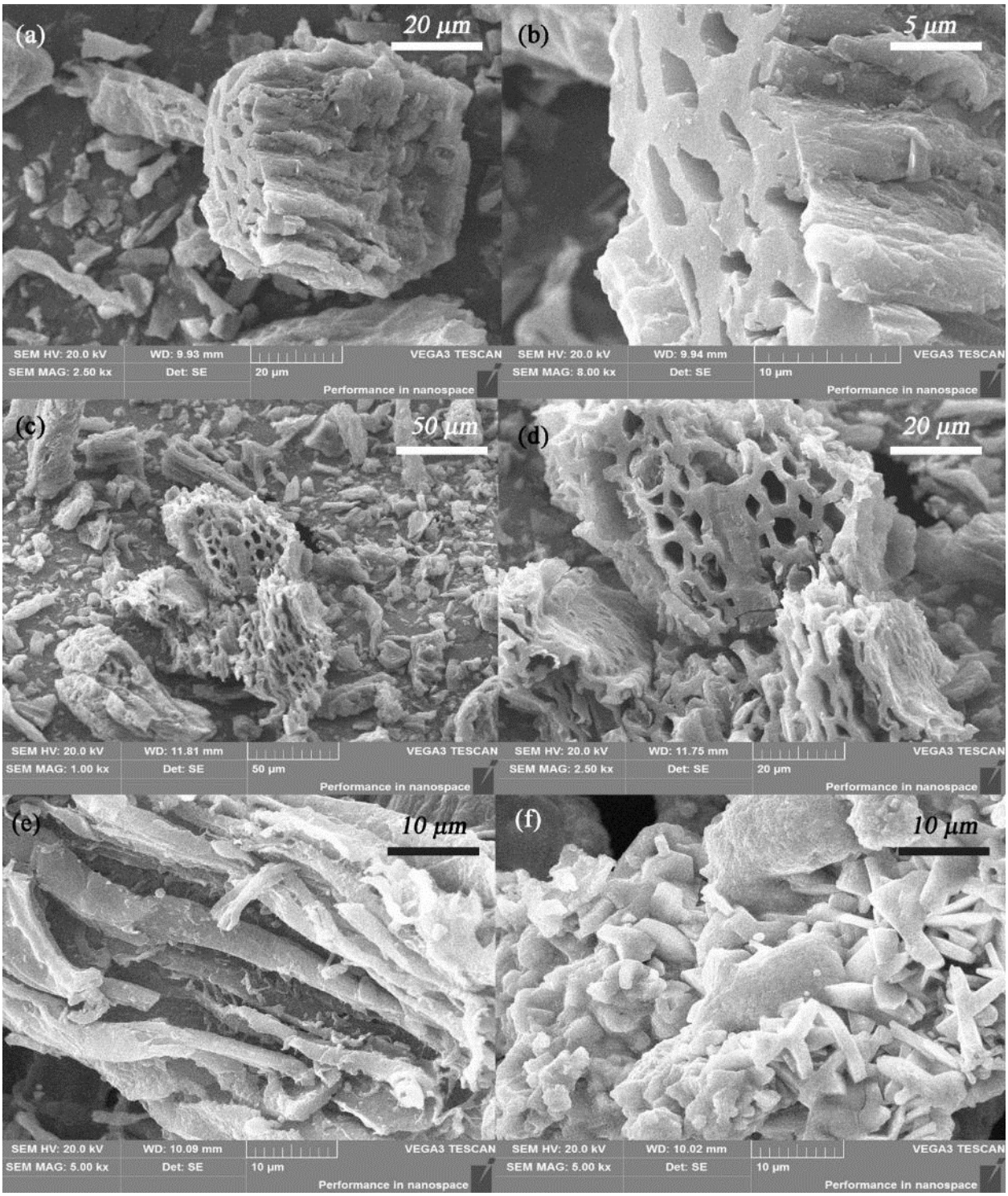

Fig. S3. SEM images of (a)-(b) N_2-GBC, (c)-(d) CO_2-GBC, (e) Cu-GBC5C and (f) Cu-GBC20C.

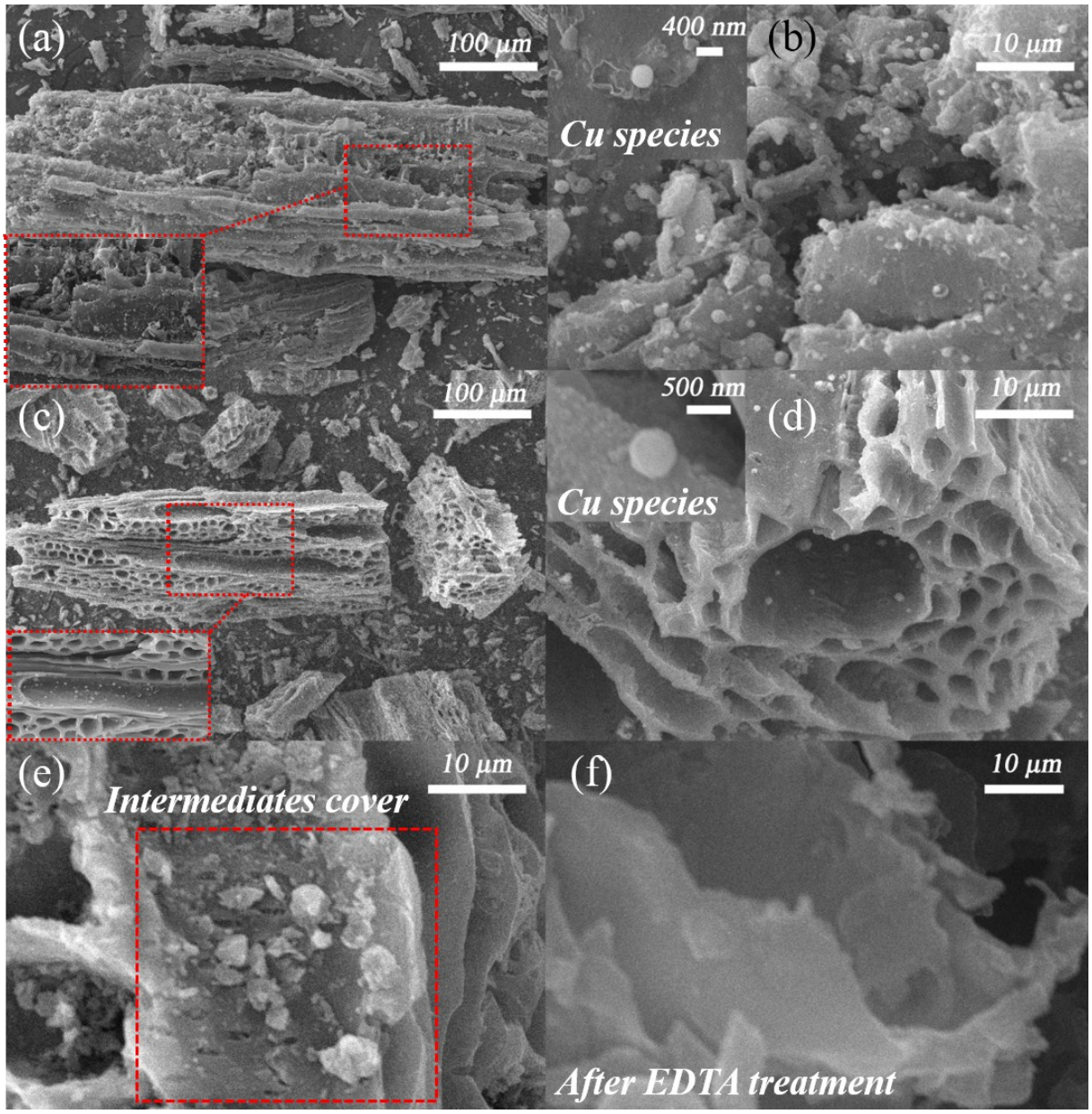

Fig. S4. SEM images of (a)-(b) Cu-GBC10N, (c)-(d) Cu-GBC10C, (e) Cu-GBC10C after one-time run batch experiments and (f) Cu-GBC10C after EDTA treatment (details in Text S4).

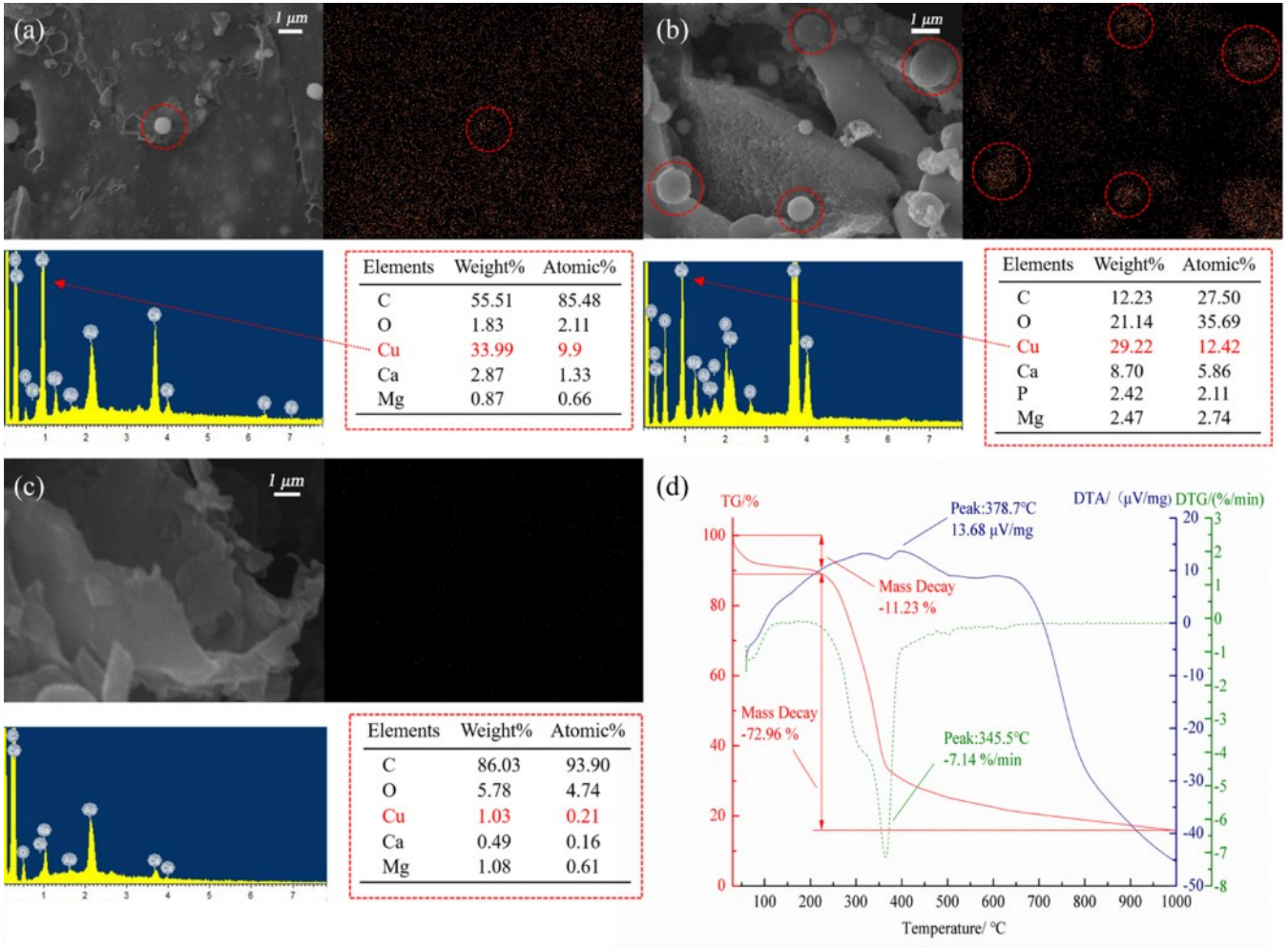

Fig. S5. EDS-Mapping images of (a) Cu-GBC10N, (b) Cu-GBC10C, (c) EDTA Cu-GBC10C and (d) TG curves of waste wood biomass

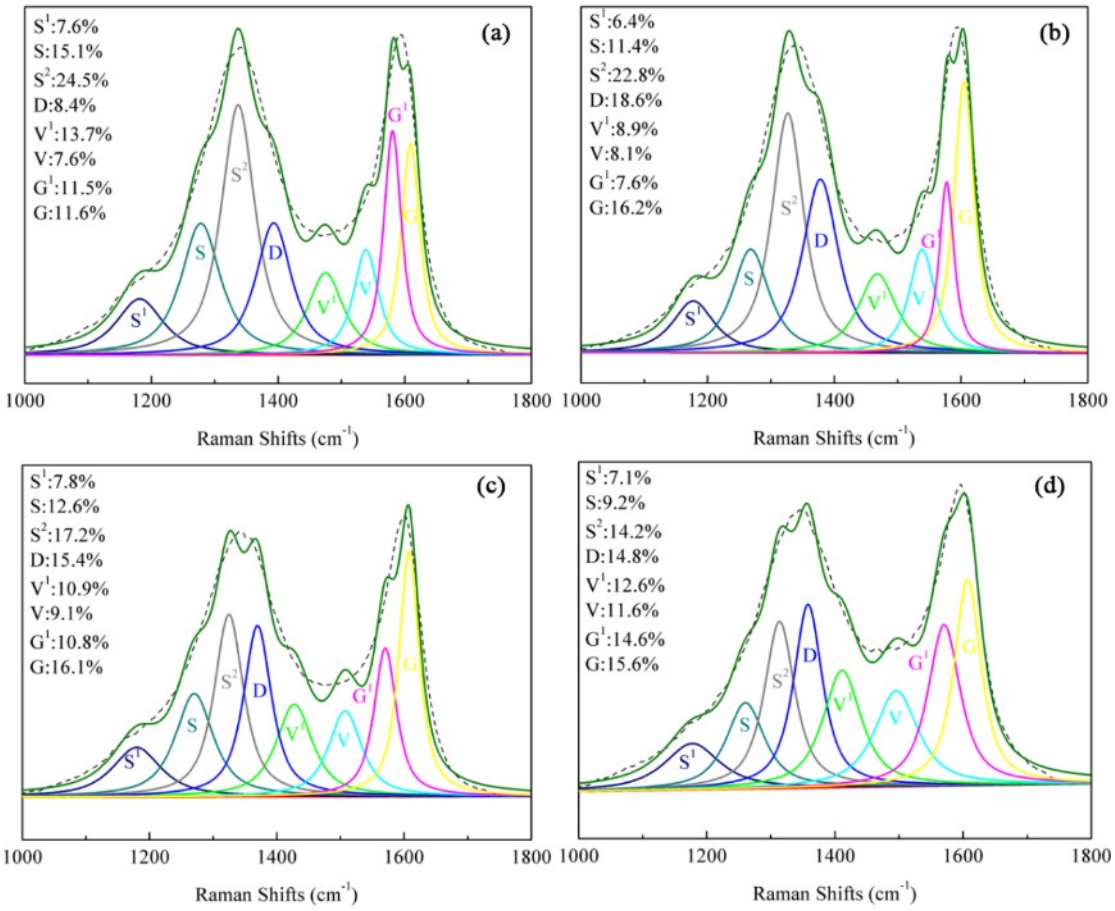

Fig. S6. Deconvoluted Raman spectrum of (a) N_2-GBC, (b) Cu-GBC10C, (c) Cu-GBC10N, and (d) Cu-GBC10C.

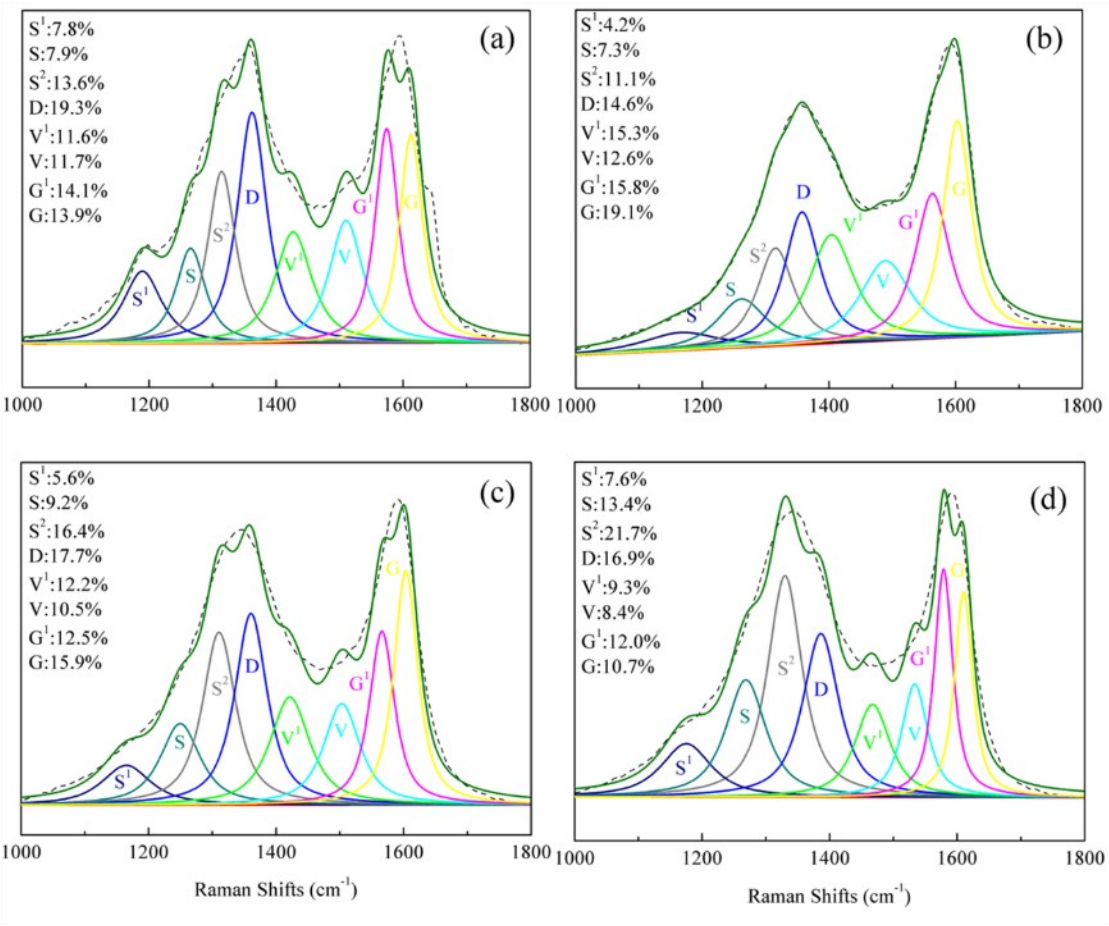

Fig. S7. Deconvoluted Raman spectrum of (a) 2nd Cu-GBC10C, (b) GO, (c) Cu-GBC5C and (d) Cu-GBC20C.

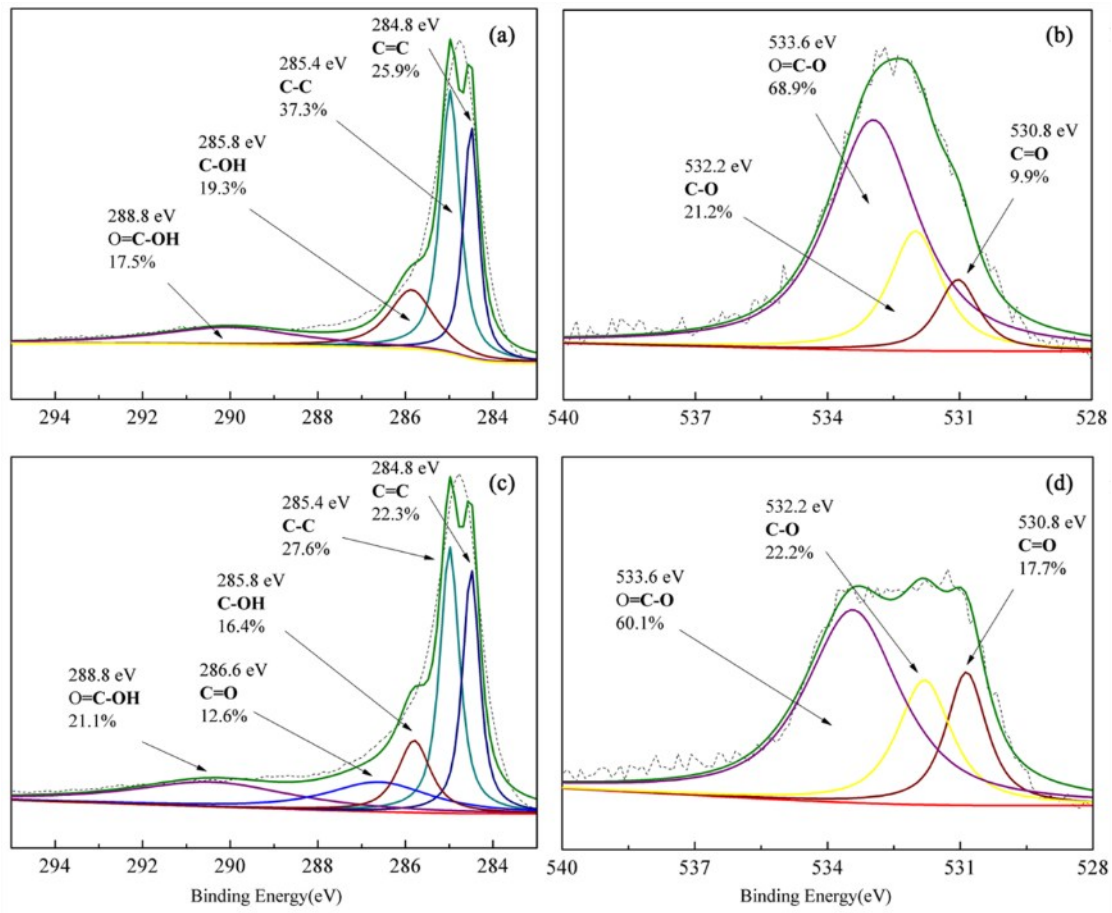

Fig. S8. Deconvoluted XPS spectrums of C 1s (O=C−OH at 288.8 eV, C=O at 286.6 eV, C−O at 285.8 eV, C−C at 285.4 eV, and C=C at 284.8 eV), O 1s (C=O at 530.8 eV, C−O at 532.2 eV, and O−C=O at 533.6eV) of (a)-(b) N_2-GBC and (c)-(d) CO_2-GBC.

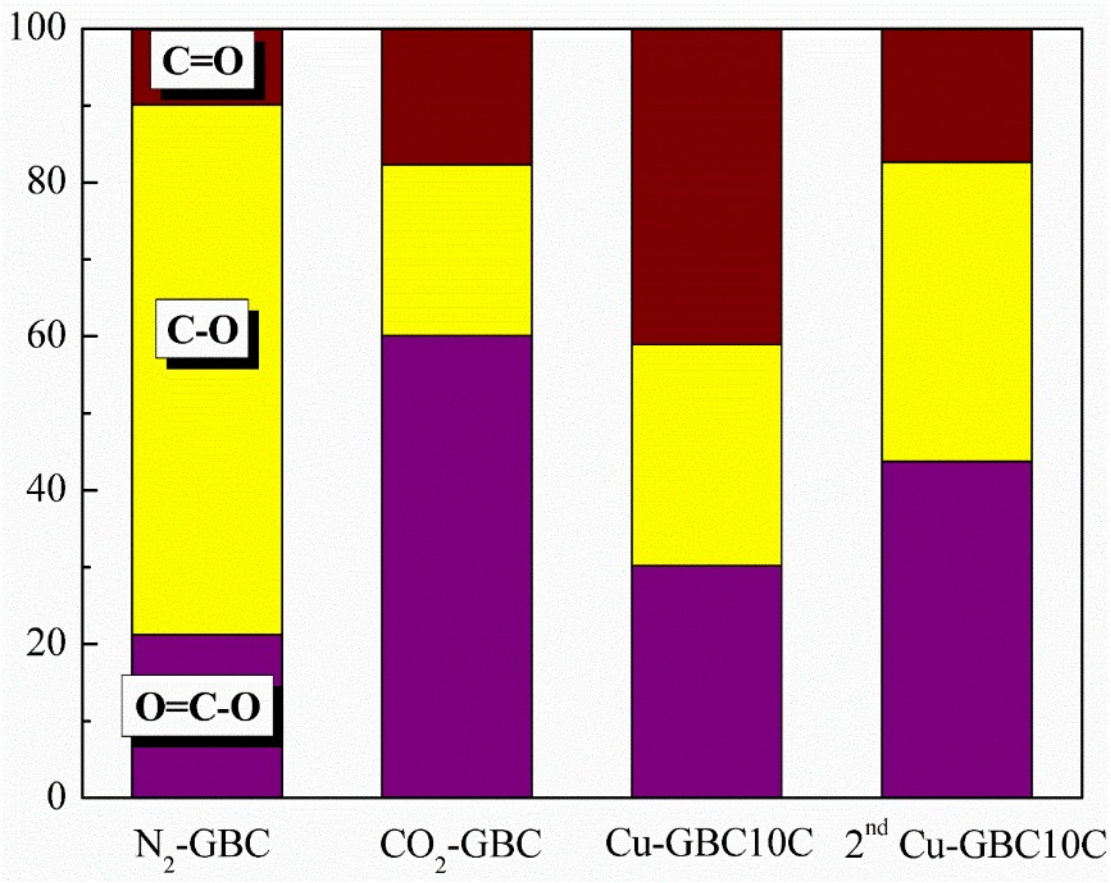

Fig. S9. Oxygen-functionalities distribution for various biochar composites.

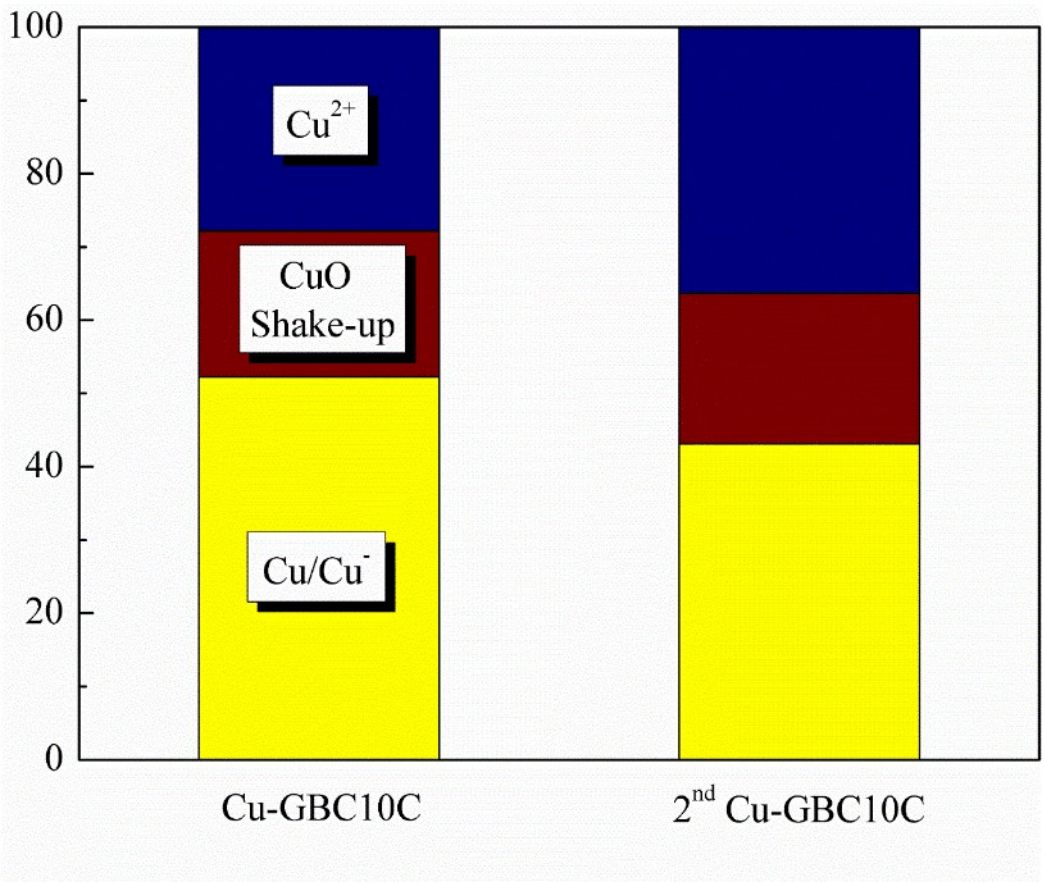

Fig. S10. Copper compositions (Cu^{2+} at 933.8 or 954.9 eV, CuO shake-up at 943.8 eV and Cu/Cu^{+} at 933.0 or 952.8eV) distribution for Cu-GBC10C before and after reaction.

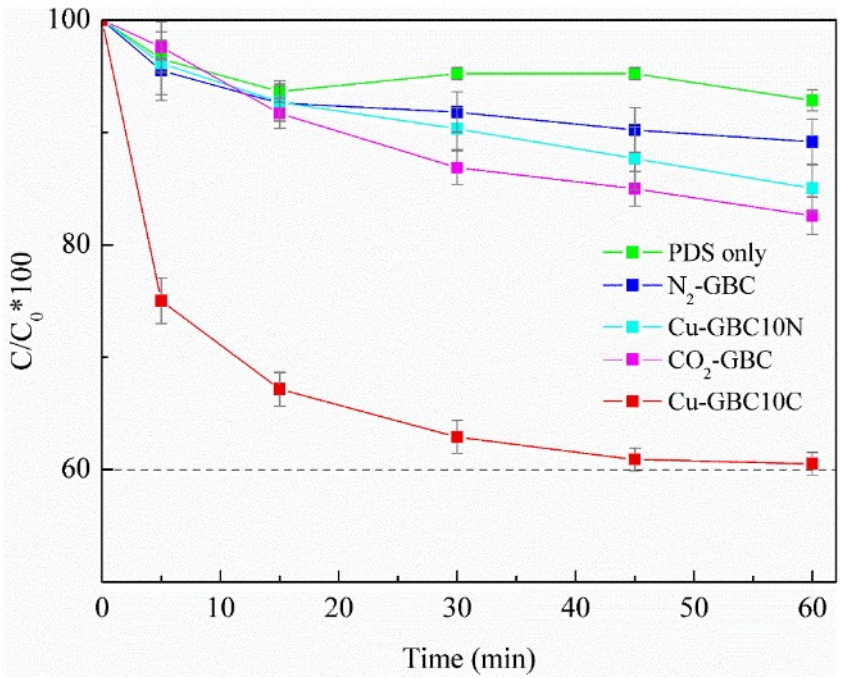

Fig. S11. Adsorption capacity of various adsorbent and PDS catalytic degradation performance ($[PDS]_0$ = 2 mM, $[adsorbent]_0$ = 0.3 g L^{-1}, $[RB]_0$ = 0.1 mM, pH = 5.8±0.2, T = 25 °C).

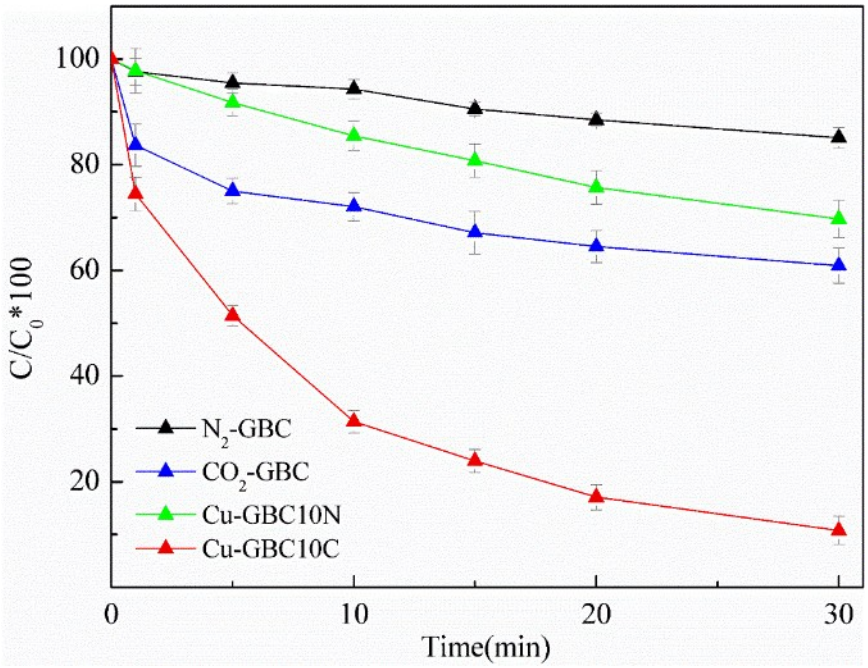

Fig. S12. RB oxidation in PDS activation process by different biochar composites ($[PDS]_0 = 2$ mM, $[BC]_0 = 0.3$ g L^{-1}, $[RB]_0 = 0.1$ mM, pH = 5.8±0.2, T = 25 °C, quenched with excess EtOH).

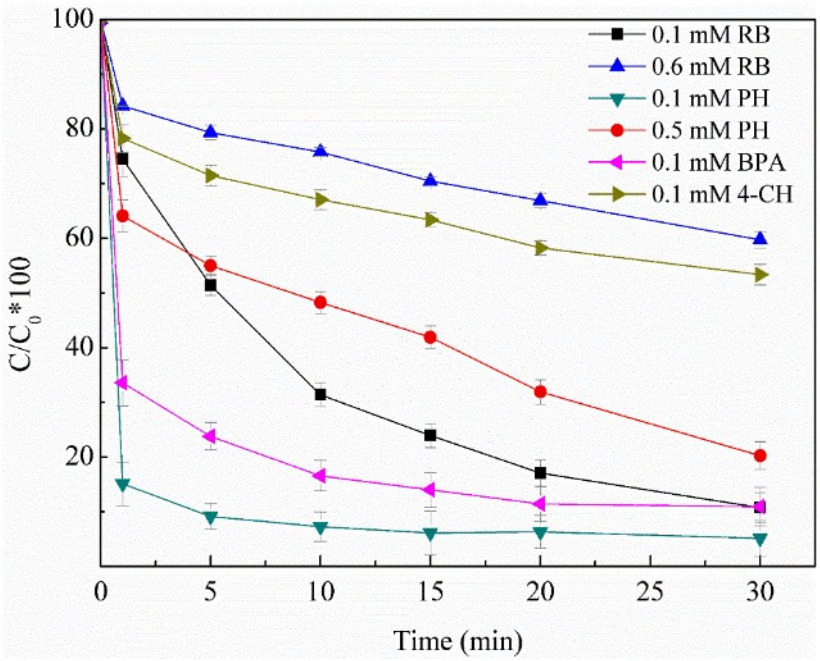

Fig. S13. Various organic pollutants (phenol, bisphenol A, rhodamine B and 4-chlorophenol) oxidation in PDS solution activated by Cu-GBC10C ($[PDS]_0$ = 2 mM, $[BC]_0$ = 0.3 g L^{-1}, pH = 5.8±0.2, T = 25 °C, quenched with excess EtOH).

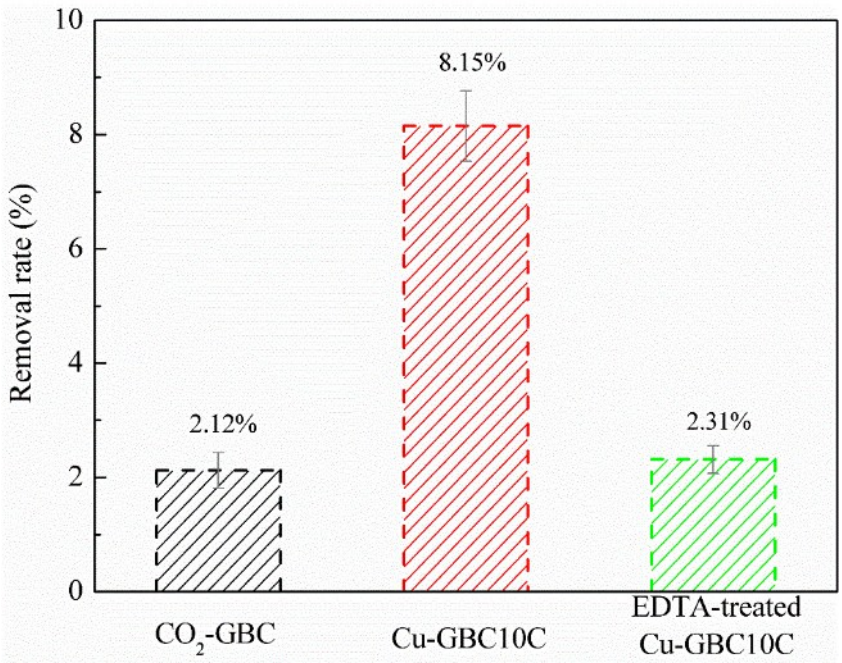

Fig. S14. Catalytic degradation performance of various catalysts after PDS pretreatment ($[PDS]_0$ = 10 mM, $[Catalyst]_0$ = 0.3 g L^{-1}, $[RB]_0$ = 0.1 mM, pH = 5.8±0.2, T = 25 °C).

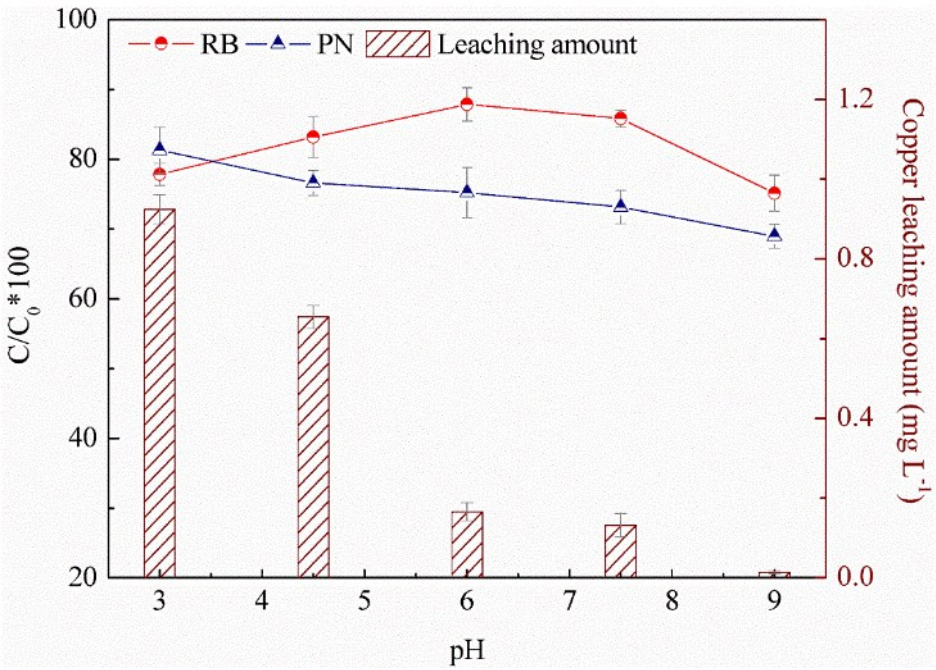

Fig. S15. Effect of pH and copper leaching amount during the pH experiments ($[PDS]_0$ = 2 mM, $[Catalyst]_0$ = 0.3 g L^{-1}, $[RB]_0$ = 0.1 mM, $[PH]_0$ = 0.5 mM, T = 25 °C).

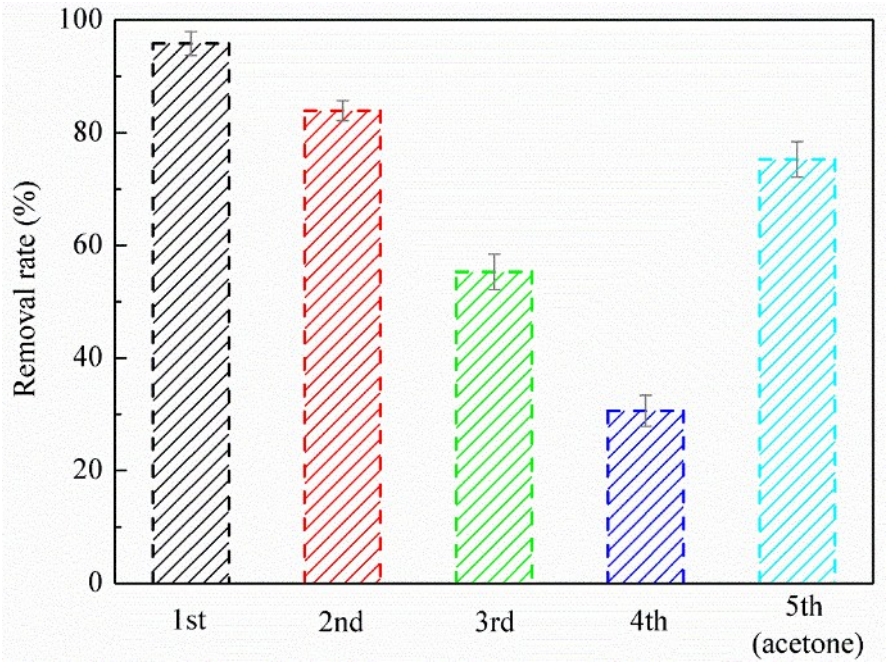

Fig. S16. Reusability and regeneration experiments employing Cu-GBC10C.

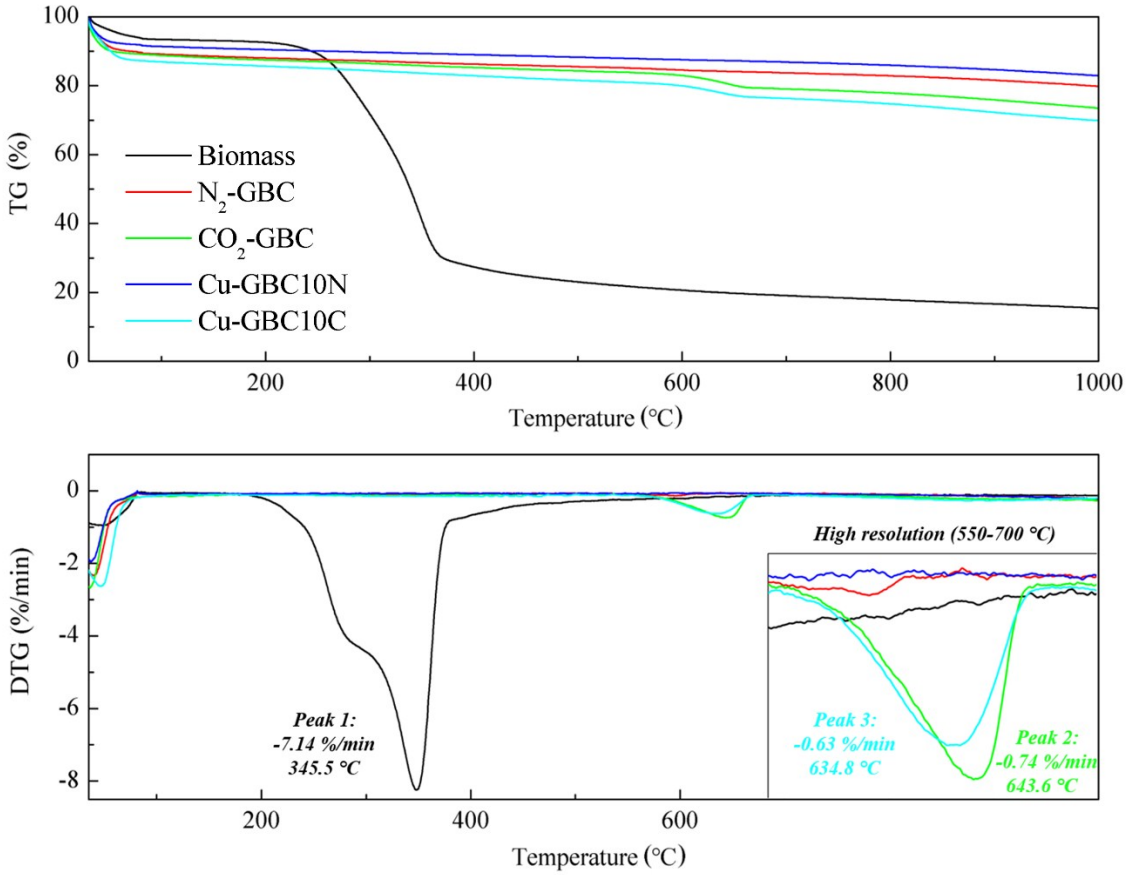

Fig. S17. TG-DTA analysis of raw biomass, N_2-GBC, CO_2-GBC, Cu-GBC10N, and Cu-GBC10C composites (temperature range 50−1000 °C, ramping rate 10 °C min^{-1}).

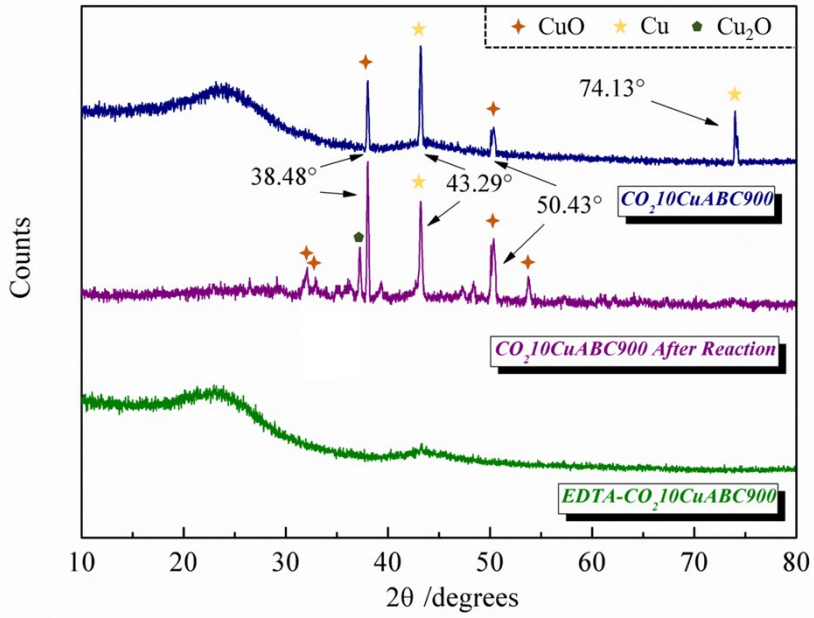

Fig. S18. XRD patterns of Cu-GBC10C, spent Cu-GBC10C after 3rd run, and EDTA Cu-GBC10C.

References

(1) Hummers, W. S.; Offeman, R. E. Preparation of Graphitic Oxide. *Journal of the American Chemical Society* **1958**, *80*, 1339-1339.

(2) Huang, D.; Luo, H.; Zhang, C.; Zeng, G.; Lai, C.; Cheng, M.; Wang, R.; Deng, R.; Xue, W.; Gong, X.; Guo, X.; Li, T. Nonnegligible role of biomass types and its compositions on the formation of persistent free radicals in biochar: Insight into the influences on Fenton-like process. *Chemical Engineering Journal* **2019**, *361*, 353-363.

(3) Liang, C.; Huang, C.-F.; Mohanty, N.; Kurakalva, R. M. A rapid spectrophotometric determination of persulfate anion in ISCO. *Chemosphere* **2008**, *73*, 1540-1543.

(4) Sun, T.; Levin, B. D. A.; Guzman, J. J. L.; Enders, A.; Muller, D. A.; Angenent, L. T.; Lehmann, J. Rapid electron transfer by the carbon matrix in natural pyrogenic carbon. *Nature Communications* **2017**, *8*, 14873.